

Super-resolution Spatial Frequency Differentiation of Nanoscale Particles with a Vibrating Nanograting

Leonid Alekseyev, Evgenii Narimanov

*Electrical and Computer Engineering Department,
Purdue University, West Lafayette, IN 47907**

Jacob Khurgin

*Electrical and Computer Engineering Department,
Johns Hopkins University, Baltimore, MD 21218*

Abstract

We propose a scheme for detecting and differentiating deeply subwavelength particles based on their spatial features. Our approach combines scattering from an ultrasonically modulated nanopatterned grating with heterodyne techniques to enable far-field detection of high spatial frequency Fourier components. Our system is sensitive to spatial features commensurate in size to the patterning scale of the grating. We solve the scattering problem in Born approximation and illustrate the dependence of the signal amplitude at modulation frequency on grating period, which allows to differentiate between model nanoparticles of size $\lambda/20$.

*Electronic address: evgenii@purdue.edu

Detection and differentiation of micro- and nanoscale particles is of great practical importance in medical and biological research, clinical diagnostics, and many other areas. Historically, optical methods have been the preferred strategy of investigating small objects, since they allow rapid, cost-effective, noninvasive analysis. As a result, a multitude of imaging and detection modalities have been developed. However, many advantages of optical detection disappear when the objects under study become substantially smaller than the wavelength, owing to the conventional $\lambda/2$ diffraction limit. This severely curtails the amount of information that can be obtained about structure, function, and composition of nanoscale particles by optical means.

In recent years, researchers have developed several approaches for optical investigation of nanoscale particles below the diffraction limit. Broadly speaking, those methods fall into one of two categories. One set of strategies aims to maximize the amount of information that can be inferred about the subwavelength objects based on aspects of scattering that are not affected by the diffraction limit. For instance, particles can be detected due to fluorescence or various other spectroscopic resonances [1]. Other approaches exploit the dependence of Rayleigh scattering intensity on particle size [2, 3]. The second category of methods involves broadening the spatial frequency passband of the system [4] by recovering evanescent waves that ordinarily cannot propagate to the far-field detector. For a number of years, this could only be achieved with optical scanning probes [5–7]. In the past decade, intense research in nanophotonics and plasmonics led to approaches towards subwavelength imaging that involve using metamaterials-based devices, which promise to be low-cost and readily adaptable for a variety of spectral regions. A negative index “superlens” [8], for instance, can transport the evanescent components of the spatial spectrum across the metamaterial slab, while also transmitting the propagating waves. However, the superlens exhibits exponential sensitivity to losses, limiting practical devices to near-field operation [9]. A more recent set of experiments involved subwavelength scatterers placed in the near field of a source. By diffracting off the scatterers, evanescent waves convert into propagating waves which could then be used to gather information about the near-field spectrum [10] or to attain subwavelength focusing [11]. However, in this far-field superlens [10], the diffracted evanescent waves mix with the existing propagating spectrum. The resulting ambiguity leads to the loss of information about the target.

In the present Letter, we propose an alternative approach to far-field detection of nanopar-

ticles, based on a device that converts evanescent waves to propagating waves via scattering on an acoustically-modulated nanograting. The salient feature of our approach is the fact that since the scattered waves are also shifted in the frequency domain, they can be easily decoupled from the existing propagating spectrum. We describe the proposed system and calculate its output signal to show that it can be used for differentiating subwavelength objects based on their size, shape, and/or composition.

The proposed detection system is shown in Fig. 1. The target object, embedded in a patterned regular array of nanorods, is illuminated with a plane wave. The spacing between the elements of the patterned array determines the resolution of the system, as well as the maximum allowable size of the target object. Because of this, the pictured device is particularly suitable for studying severely subwavelength targets. The nanorods are made to vibrate using a high-frequency piezoelectric transducer. Ultrasonic devices reaching 10 GHz are within reach of contemporary technology [12, 13], making it possible to achieve frequency shifts exceeding the linewidth of a narrowband optical source.

Due to patterning and ultrasonic modulation, the dielectric function of the nanorod array is periodic both in space and time. In the space domain it can be represented as a Fourier series with large wave vectors ($q \gg 2\pi/\lambda$). Thus, components of the incident radiation that scatter from subwavelength features of the target and are now evanescent (due to acquiring large transverse wave vectors) can scatter again from the nanorod array, reducing their transverse wave vector. As such, these fields can retain their propagating nature while carrying subwavelength information. Now, because of the periodic time dependence of the nanorod permittivity (which we write as $\epsilon = \bar{\epsilon} + \delta\epsilon(\mathbf{r} - \boldsymbol{\eta} \cos \Omega t)$, with $\boldsymbol{\eta}$ being the amplitude and Ω the frequency of the ultrasonic vibration), the frequency of these scattered signals is shifted by Ω , thereby separating them out from the rest of the propagating waves and allowing their unique retrieval.

To analyze the proposed system, we will consider the Green's function solution of time-harmonic Maxwell's equations. For simplicity, we treat a system that is translationally invariant in the direction of the cylindrical nanorods, perfectly aligned along the z axis. The target objects are also assumed to have infinite extent in the z direction. Further, we assume that the spatial dimensions and/or the index contrast of the scattering system are small. In

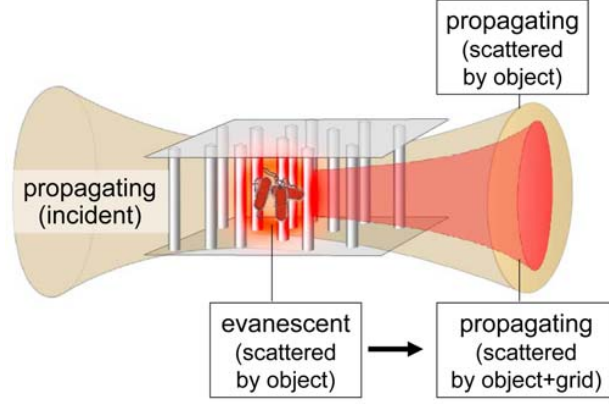


FIG. 1: Schematics of the proposed system. Evanescent components of radiation from the sample scatter from the nanostructure and propagate into the far field. Vibration of the nanorods leads to a frequency shift which enables detection of these evanescent contributions using lock-in techniques.

this case, the solution to Maxwell's equations can be represented by the Born series

$$\begin{aligned}
E(\mathbf{r}) = & E_0(\mathbf{r}) + \left(\frac{\omega}{c}\right)^2 \int G(\mathbf{r}, \mathbf{r}') \delta\epsilon(\mathbf{r}) E_0(\mathbf{r}') d\mathbf{r}' + \\
& + \left(\frac{\omega}{c}\right)^4 \int G(\mathbf{r}, \mathbf{r}') \delta\epsilon(\mathbf{r}) \int G(\mathbf{r}', \mathbf{r}'') \delta\epsilon(\mathbf{r}'') E_0(\mathbf{r}'') d\mathbf{r}'' d\mathbf{r}' \quad (1) \\
& + O((\delta\epsilon)^3),
\end{aligned}$$

where $E_0(\mathbf{r}) = \exp(i\mathbf{k} \cdot \mathbf{r})$ and $G(\mathbf{r}, \mathbf{r}') \sim H_0^{(1)}(k|\mathbf{r} - \mathbf{r}'|)$ is the usual Green's function for a 2D Helmholtz equation, proportional to the Hankel function, and $\delta\epsilon(\mathbf{r}) = \epsilon(\mathbf{r}) - \overline{\epsilon(\mathbf{r})}$ serves as a weak scattering potential. We retain the second order term in the Born series because this is the lowest order in which the acoustically-shifted signal at frequency $\omega + \Omega$ is in the propagation band of the system. Separating the scattering potential into contributions from the grid and from the target ($\delta\epsilon = \delta\epsilon_{\text{gr}} + \delta\epsilon_{\text{t}}$), we can decompose Eq. (1) into terms corresponding to the different scattering processes:

$$E(\mathbf{r}) \equiv E_0(\mathbf{r}) - \frac{i}{4} \left(\frac{\omega}{c}\right)^2 (I_{\text{gr}} + I_{\text{t}}) - \frac{1}{16} (I_{\text{gr-gr}} + I_{\text{t-t}} + I_{\text{gr-t}} + I_{\text{t-gr}}). \quad (2)$$

Here, terms of the form I_x and I_{x-y} stand for Green's function integrals expressing the contributions to the total field due to single and double scattering. In particular,

$$I_{x-y} = \iint \delta\epsilon_x(\mathbf{r}') \delta\epsilon_y(\mathbf{r}'') H_0^{(1)}(k|\mathbf{r} - \mathbf{r}'|) H_0^{(1)}(k|\mathbf{r}' - \mathbf{r}''|) \exp(i\mathbf{k} \cdot \mathbf{r}'') d\mathbf{r}'' d\mathbf{r}'. \quad (3)$$

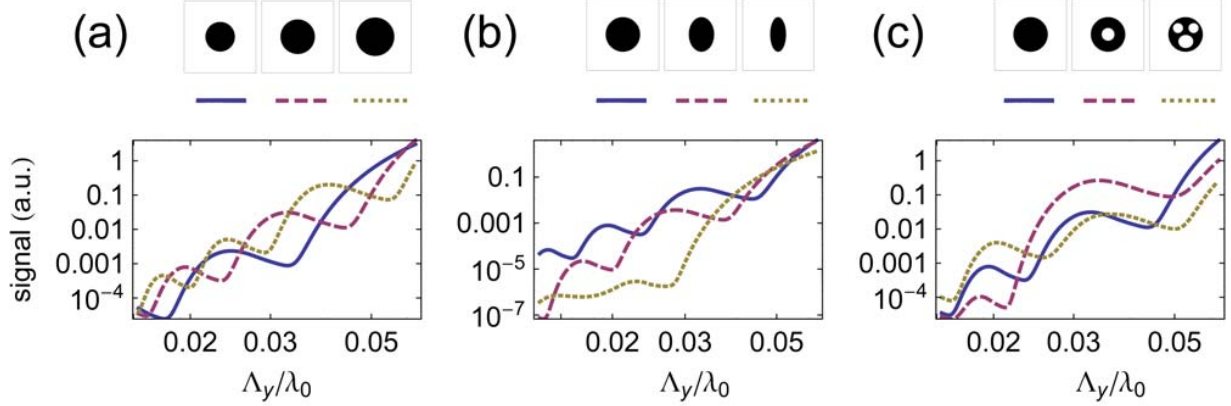


FIG. 2: Simulated signal as a function of grating period in the y direction as size, shape, and structure [panels (a), (b), and (c) respectively] of the model target (cylinder with $d = \lambda/20$) are altered. Different line types (solid, medium dashed, fine dashed) correspond to the different target cross sections, as illustrated.

The important terms in Eq. (2) are $I_{\text{gr-t}}$ and $I_{\text{t-gr}}$. The fields corresponding to those terms carry information about the high spatial frequency components of the target objects that have been downshifted into the propagation band of the system and, furthermore, have been “tagged” with the modulation frequency of the grid. Interference between these shifted signals at frequency $\omega \pm \Omega$ with the illuminating wave allows to retrieve the information through lock-in detection (provided the modulation frequency Ω is used as a reference). When we put in an explicit expression for a vibrating grid, both terms lead to the same expression:

$$I_{\text{gr-t}} \sim \frac{e^{ikr}}{\sqrt{kr}} \sum_{m=-\infty}^{\infty} e^{im\Omega} \left[\sum_{\mathbf{q}_n} i^m J_m(\mathbf{q}_n \cdot \boldsymbol{\eta}) \text{jinc} \left(\frac{aq_n}{2\pi} \right) \frac{\delta\epsilon_t(\mathbf{k}_{\text{obs}} - \mathbf{k} - \mathbf{q}_n)}{q_n^2 - 2\mathbf{k}_{\text{obs}} \cdot \mathbf{q}_n} \right]. \quad (4)$$

Here, the following assumptions have been made: the grid is composed of a regular 2D array of cylindrical rods with radius a and spacing Λ ($a < \Lambda \ll \lambda$); $\mathbf{q}_n \sim 1/\Lambda$ are the grid reciprocal lattice vectors, $\text{jinc}(r) \equiv J_1(2\pi r)/\pi r$, $\mathbf{k}_{\text{obs}} \equiv k\hat{\mathbf{r}}$ is a propagation vector aligned with the detector, and m is the diffraction order. Since the detector is assumed to be in the far field, Hankel asymptotics were used.

In addition, we expect a realistic sample to contain many target objects randomly distributed in the nanorod grid and randomly oriented. As a result, the Fourier representation of the dielectric function $\delta\epsilon_t(\mathbf{q})$ will contain a sum over the phase factors corresponding

to optical path length difference between the scatterers. Because the relative positions of the scatterers are random, these phase factors form a mean zero distribution. Due to the finite integration time at the detector, as well as its finite aperture, the average contribution from the random phases can be shown to approach zero [14]. Taking $m = 1$ in Eq. (4) and squaring to compute the intensity signal, we obtain the following expression for the detected signal at frequency Ω :

$$|A|^2 \propto N \sum_{\mathbf{q}}' \left| \mathbf{q} \cdot \boldsymbol{\eta} \text{jinc} \left(\frac{aq}{2\pi} \right) \frac{\delta\epsilon_t^{\text{av}}(q)}{q^2} \right|^2 + O \left(\frac{N}{\sqrt{T}} \right), \quad (5)$$

where N is the number of target objects, T is the integration time, and $\delta\epsilon_t^{\text{av}}(q)$ is the angular average (due to random orientations) of the spacial frequency representation of an individual target.

To illustrate the ability of the proposed system to distinguish between subwavelength particles, in Fig. 2 we plot the signal computed from Eq. (5) as a function of the grating period in the y direction (Λ_y). In order to achieve effective tunability of this period in a physical device, it could be manufactured as a chirped grid in which the local period varies slowly on the scale of the wavelength. (Within the effective scattering volume, the local period should be approximately constant; any imperfections in the grid will decrease device performance.) Note that it would be sufficient to vary the period along one direction only; in the other direction the nanorod spacing could be arbitrary. In particular, it could be made large enough to allow objects to be translated in the device, e.g. via microfluidics.

As a basic model target, we take a cylinder with diameter $\lambda/20$, well below the diffraction limit. We then explore how the computed signal differs as we perturb the target's size, shape, and as we introduce some inner structure to the particle [panels (a), (b), and (c) of Fig. 2]. The abscissas indicate the local period of the nanostructure in the y direction in units of $1/\lambda$. The curves, plotted on the log-log scale, illustrate the differences between signals for the different conformations of our model particle, depicted above the panels. The secular trend of the curves indicates a power law decrease of the signal as spatial frequencies increase.

The clear differences between the curves in each panel of Fig. 2 suggest that changes in either the size, shape, or structure of the targets on a deeply subwavelength scale can be detected with our proposed approach. We note, however, that due to angular averaging over multiple randomly oriented targets, this scheme is sensitive only to the average radial

spatial frequency distributions in the sample, which are not necessarily unique. Thus, these signals do not provide unambiguous signatures for arbitrary targets. However, even with this limitation it should be possible to extract useful information given some prior knowledge about the sample under study. For instance, given a mixture containing the differently-sized particles of Fig. 2(a), we could provide an estimate of the size of the smallest component in the mixture by observing the location of the first minimum of the signal as the period Λ_y decreases. Similarly, for a circle/ellipsoid family of Fig. 2(b), we could estimate the eccentricity of the “narrowest” ellipsoid.

If it is known that only *one* out of a set of possible targets is present, its identity could be revealed by comparing the data to known calibration signals.

Finally, we can also imagine other experiments, in which the shape or structure of the target is changing in real time under the influence of some external mechanism (e.g. mitochondria undergoing calcium overload [15] or cells undergoing apoptosis [16]). Looking at the curves of Fig. 2(b) it’s easy to see that as the ellipsoidal targets become deformed into spheres (a good model for the calcium-induced alterations in mitochondrial morphology [15]), the signal changes rather dramatically. Thus, the proposed system could be used to detect real-time target morphology changes on a deeply subwavelength scale.

In conclusion, we have proposed a system that enables differentiation of nanoscale particles by their sub-diffraction-limited spatial spectrum components, which can be detected in the far field by utilizing scattering from an ultrasonically modulated grating. We note that the model system treated here is one out of many possible configurations, and that many potential implementations exist, including layered planar systems. Compared to existing techniques, our scheme allows to create a much richer spatial frequency fingerprint for nanoscale objects.

-
- [1] S. W. Hell, *Science* (New York, N.Y.) **316**(5828), 1153 (May 2007).
 - [2] G. G. Daaboul, A. Yurt, X. Zhang, G. M. Hwang, B. B. Goldberg, and M. S. Unlu, *Nano letters* (Oct. 2010).
 - [3] F. Ignatovich and L. Novotny, *Physical Review Letters* **96**(1), 1 (Jan. 2006).
 - [4] Y. Kuznetsova, A. Neumann, and S. R. J. Brueck, *Opt. Express* **15**, 6651 (2007).

- [5] B. Dragnea, J. Preusser, J. M. Szarko, S. R. Leone, and W. D. J. Hinsberg, *J. Vac. Sci. Technol. B* **19**, 142 (2001).
- [6] B. Knoll and F. Keilmann, *Nature* **399**, 134 (1999).
- [7] N. C. J. van der Valk and P. C. M. Planken, *Appl. Phys. Lett.* **81**, 1558 (2002).
- [8] J. B. Pendry, *Phys. Rev. Lett.* **85**, 3966 (2000).
- [9] V. A. Podolskiy and E. E. Narimanov, *Opt. Lett.* **30**, 75 (2005).
- [10] S. Durant, Z. Liu, J. M. Steele, and X. Zhang, *Journal of the Optical Society of America B* **23**(11), 2383 (2006).
- [11] G. Lerosey, J. de Rosny, A. Tourin, and M. Fink, *Science* **315**, 1120 (2007).
- [12] R. Lanz and P. Muralt, *IEEE transactions on ultrasonics, ferroelectrics, and frequency control* **52**(6), 936 (Jun. 2005).
- [13] M. B. Assouar, O. Elmazria, P. Kirsch, P. Alnot, V. Mortet, and C. Tiusan, *Journal of Applied Physics* **101**(11), 114507 (2007).
- [14] L. V. Alekseyev, *Non-magnetic Optical Metamaterials: Fundamentals and Applications*, Ph.D. thesis, Princeton University (2011).
- [15] N. N. Boustany, R. Drezek, and N. V. Thakor, *Biophysical journal* **83**(3), 1691 (Sep. 2002).
- [16] C. S. Mulvey, A. L. Curtis, S. K. Singh, and I. J. Bigio, *IEEE Journal of Selected Topics in Quantum Electronics* **13**(6), 1663 (2007).